Acta Medica Okayama

Volume 47, *Issue* 3 1993 *Article* 4

JUNE 1993

Quantitative measurement of normal and hydrocephalic cerebrospinal fluid flow using phase contrast cine MR imaging.

Shinji Katayama* Shoji Asari†

Takashi Ohmoto‡

*Okayama University,

†Okayama University,

‡Okayama Univerisity,

Quantitative measurement of normal and hydrocephalic cerebrospinal fluid flow using phase contrast cine MR imaging.*

Shinji Katayama, Shoji Asari, and Takashi Ohmoto

Abstract

Measurements of the cerebrospinal fluid (CSF) flow using phase contrast cine magnetic resonance (MR) imaging were performed on a phantom, 12 normal subjects and 20 patients with normal pressure hydrocephalus (NPH). The phantom study demonstrated the applicability of phase contrast in quantitative measurement of the slow flow. The CSF flows of the normal subjects showed a consistent pattern with a to-and-fro movement of the flow in the anterior subarachnoid space at the C2/3 level, and they were dependent on the cardiac cycle in all subjects. However, the patients with NPH showed variable patterns of the CSF pulsatile flow and these patterns could be divided into four types according to velocity and amplitude. The amplitudes of each type were as follows: type 0 (n = 1), 87.6mm; type I (n = 2), 58.2mm (mean); type II (n = 6), 48.0 +/- 5.0mm (mean +/- SEM); and type III (n = 11), 19.9 +/- 1.8mm (mean +/- SEM). The decrease of the amplitudes correlated to a worsening of the clinical symptoms. After the shunting operation, the amplitude of to-and-fro movement of the CSF increased again in the patients with NPH who improved clinically. Some of the type III cases were reclassified type II, I and 0 and also one of the type II cases changed type I after the shunting operation. We conclude that the phase contrast cine MR imaging is a practically and clinically applicable technique for the quantitative measurement of the CSF flow.

KEYWORDS: cerebrospinal fluid flow, normal pressure hydrocephalus, magnetic resonance imaging, phase contrast

---

*PMID: 8379344 [PubMed - indexed for MEDLINE]

Acta Med Okayama 47 (3) 157-168 (1993)

Quantitative Measurement of Normal and Hydrocephalic Cerebrospinal Fluid Flow Using Phase Contrast Cine MR Imaging

Shinji Katayama*, Shoji Asari and Takashi Ohmoto

Department of Neurological Surgery, Okayama University Medical School, Okayama 700, Japan

Measurements of the cerebrospinal fluid (CSF) flow using phase contrast cine magnetic resonance (MR) imaging were performed on a phantom, 12 normal subjects and 20 patients with normal pressure hydrocephalus (NPH). The phantom study demonstrated the applicability of phase contrast in quantitative measurement of the slow flow. The CSF flows of the normal subjects showed a consistent pattern with a to-and-fro movement of the flow in the anterior subarachnoid space at the C2/3 level, and they were dependent on the cardiac cycle in all subjects. However, the patients with NPH showed variable patterns of the CSF pulsatile flow and these patterns could be divided into four types according to velocity and amplitude. The amplitudes of each type were as follows: type 0 (n = 1) , 87.6mm; type I (n = 2), 58.2mm (mean); type II (n = 6), 48.0 ± 5.0mm (mean ± SEM); and type III (n = 11), 19.9 ± 1.8mm (mean ± SEM). The decrease of the amplitudes correlated to a worsening of the clinical symptoms. After the shunting operation, the amplitude of to-and-fro movement of the CSF increased again in the patients with NPH who improved clinically. Some of the type III cases were reclassified type II, I and 0 and also one of the type II cases changed type I after the shunting operation. We conclude that the phase contrast cine MR imaging is a practically and clinically applicable technique for the quantitative measurement of the CSF flow.

Key words : **cerebrospinal fluid flow, normal pressure hydrocephalus, magnetic resonance imaging, phase contrast**

Dumoulin *et al.* (1-6) has reported phase contrast to be a practically and clinically applicable technique for the imaging and quantitatively measuring of the blood flow. Although this technique for imaging is used in MR angiography (1-5, 7, 8), reports of the applications of this technique in quantitative measurement are few (6, 9, 10). The purpose of the present study is to show some practical and clinical applications of phase contrast cine MR imaging for the quanitatative measurement of the cerebrospinal fluid (CSF) flow.

We clinically applied this technique in patients with normal pressure hydrocephalus (NPH). Ever since Adams and Hakim (11) described NPH as a surgically treatable dementia, many authors have investigated this condition with various methods such as cisternography, computerized tomography (CT) scanning (12-14), intracranial pressure (ICP) monitoring(13, 15, 16) and cerebral blood flow measurements (17). With the advent of MR imaging, Sherman *et al.* (18-20) initially reported a CSF flow-void sign for the qualitative analysis of normal CSF pulsatile flow. Previous MR studies (21-29) reported the increase in the CSF flow void sign as one of the characteristics of NPH. However, the pathophysiology of NPH is complicated and many questions remain to be solved.

This study is divided into three main parts. The first part of this study is calibration of the steady flow phantom. The second is practical studies on normal volunteers. The third is clinical applications on patients with NPH.

* To whom correspondence sholud be addressed.

Subjects and Methods

Phantom study. The phantom consisted of a vinyl tube (9 mm inner diameter) filled with saline and a plastic basin filled with micromolecular dextran. The tube was connected to a pump for circulation and to a electromagnetic flow meter for the measurement of flow rates.

Normal subjects. Twelve healthy volunteers (2 women and 10 men) were studied in the present study. These subjects ranged in age from 13 to 63 (mean of 31 years).

NPH patients. Twenty patients with ventricular dilatation (12 women and 8 men, aged 28 to 80 years; mean age of 63 years) were studied in the present study.

All patients had some clinical symptoms, symmetrical ventricular dilatation on CT and abnormal findings such as ventricular reflux within 6 h and/or ventriculr stasis after 24 h on CT- or isotope-cisternography. However, lumbar CSF pressures were normal ($< 180\,mmH_2O$) in all patients and they were all suspected of having NPH. All patients were summarized in Table 1. Patients with abnormal spinal lesions such as disc herniation, canal stenosis or tumor were excluded in the present study. The patients were neurologically examined by more than two neurological surgenos and in all patients, NPH score (16) was measured in evaluating clinical disabilities before and after the shunting operation. The following scale was used to evaluate the three main symptoms of NPH. Minor symptoms such as headache and/or mild mental disorder were excluded in this scale. The minimum possible score was 3 points and the maximum was 15 points.

a) Gait evaluation: 1 point if the patient is bedridden or not able to walk; 2, if ambulation is possible with help; 3, when independent walking is possible but is unstable or the patient falls; 4, if abnormal but stable gait present; and 5 point when gait is normal.

b) Cognitive function: 1 point when patient is vegetative; 2, if severe dementia is present; 3, when important memory problems exist with more or less severe behavior disturbances; 4, when memory problems exist that are reported by patient or family; and 5, when only cognitive disturbances are found by specific tests.

c) Sphincter disturbance: 1, when the patients both urinary and fecal incontinence; 2, if continuous urinary incontinence is present; 3, when sporadic urinary incontinence exists; 4, only urinary urgency is present; and 5, when there are no objective nor subjective sphincter dysfuntion.

Additionally, Evans' index on CT as a ventricular size was measured. Periventricular low density (PVL) on CT was also observed in all patients before the shunting operation. Postoperative NPH scores were measured at the time of the postoperative MR imagings of the CSF flow. The average time between the operation and the postoperative MR imaging was one month.

Table 1 Summary of patients with normal pressure hydrorephalus

Case No.	Age /Sex	Etiology	NPH score				Evans' index	PVL	Lumbar CSF pressure (mmH_2O)	TVFP type	Surgical treatment	Outcome
			GE	CF	SD	total						
1	73/F	SAH	3	2	2	7	40	+	130	0	/	—
2	80/M	Unknown	3	3	3	9	37	+	120	I	/	—
3	65/M	Unknown	2	2	1	5	33	+	120	I	VP shunt	Effective
4	28/F	Unknown	5	5	5	15	29	—	120	II	/	—
5	67/F	SAH	2	4	5	11	31	+	70	II	/	—
6	54/F	SAH	5	5	5	15	24	—	150	II	/	—
7	74/F	SAH	1	2	1	4	40	+	130	II	VP shunt	Effective
8	64/M	Trauma	2	3	1	6	36	+	80	II	VP shunt	Effective
9	69/M	Trauma	1	2	1	4	36	+	100	II	VP shunt	Effective
10	78/M	Trauma	1	2	1	4	30	+	160	III	/	—
11	65/F	SAH	1	2	1	4	39	+	130	III	VP shunt	Effective
12	72/F	Unknown	1	3	1	5	38	+	125	III	VP shunt	Effective
13	44/F	SAH	1	2	1	4	43	+	120	III	VP shunt	Effective
14	43/M	SAH	2	2	1	5	32	—	120	III	VP shunt	Effective
15	74/F	SAH	1	2	1	4	34	+	180	III	VP shunt	Effective
16	46/M	Unknown	1	2	1	4	45	—	160	III	VP shunt	Effective
17	57/M	Trauma	1	2	1	4	37	—	180	III	VP shunt	NE
18	70/F	Unknown	1	2	1	4	54	—	80	III	VP shunt	NE
19	66/F	Trauma	1	2	1	4	39	+	120	III	VP shunt	Effective
20	78/F	Unknown	2	3	3	8	30	+	120	III	VP shunt	Effective

GE: gait evaluation, CF: cognitive function. SD: sphincter disturbance.
PVL: periventricular low density, TVFP: time-velocity flow profile, SAH: subarachnoid hemorrhage
+: positive, −: negative, /: not perfomed, NE: not effective

MR imaging. A 0.5 tesla (T) clinical MR system (Resona, Yokogawa Medical Systems, Tokyo, Japan) was used for all imaging. The bipolar flow-encoding gradient pulse sequence [time of repetition (TR) determined by the subject's R-to-R interval/20/4] [TR/time of echo (TE)/excitations] utilizing a cardiac gate was used. Flip angle was at 30 degrees. The image matrix was 160×192, the field of view was 20 cm and the slice thickness was 5 mm. The bipolar flow-encoding gradient pulse was applied along the cranial to caudal direction. We used a bird-cage shaped head-coil to transmit and receive the signals. Eight to 12 phase images in the midsagittal plane of the brain and the upper cervical spine were acquired during each cardiac cycle. The first phase image was acquired at 10 msec after the R-wave on ECG and the rest of the images were sequentially imaged with 60 msec intervals. The total examination time was approximately 5–10 min using this sequence. When the modulations of the phase shift were between 0 and $\pm \pi$, then the iso-high signal intensities represented the cephalic CSF flow and the iso-low signal intensities represented the caudal CSF flow on phase images.

Measurement of CSF Flow Velocity

Theoretical background. Phase images are obtained by complex subtraction of the two data sets that are acquired by applying the bipolar flow-encoding gradient pulse along the flow direction. The polarity of the bipolar pulse is reversed on alternate acquisitions. This reversal sequentially cancels the phase shift of the stationary protons but does not cancel the phase shift of the moving protons along the axis of the gradient. The two sets of data on the stationary protons are identical in signal, but the signal from the moving protons are different. Therefore, only the subtraction from the stationary protons are canceled on complex subtraction. The phase shift φ induced by the bipolar flow-encoding pulse is $\varphi = \gamma VTAg + \gamma AT^2Ag$, where γ is the gyromagnetic ratio, V is the velocity component in the flow encoded direction, T is the time interval between the centers of the two lobes. Ag is the area of one lobe of the bipolar pulse and A is acceleration (4). In the present study, we used 0.005 sec as T. Therefore, T^2 was a very small number and $\gamma VTAg + \gamma AT^2Ag$ was considered to be nearly equal to $\gamma VTAg$ in the present study. In this equation, the phase shift is proportional to the magnitude of the flow-encoding gradient and the velocity. If the magnitude of the flow-encoding gradient is fixed, the phase shift will be directly proportional to the velocity. The magnitude of the bipolar flow-encoding gradient is determined by the value of the encoded (velocity encoding) in our MR system. The relationship between the signal and the phase shift is sinusoidal. Therefore, if the phase shift is less than the radian at the maximum velocity, the velocity V will be detected directly from the signal intensities in the phase images with the following equation. The velocity (V) is V = velocity encoding $\times$ (SIR − SIB)/500π, where SIR is the signal intensity in the region of interest (ROI), SIB is the signal intensity in the background and 500π is the specific number in our MR system.

Time-velocity flow profile (TVFP) The CSF flow velocity was measured in the anterior subarachnoid space at the C2/3 level in all subjects. Round ROIs (0.02 cm^2) were defined on sagittal images in the present study. We used CSF velocity profiles (time-velocity flow profile, TVFP) to define the pattern of the to-and-fro movement of the CSF flow.

Results

Velocity encoding. Since we had to determine the sensitive velocity encodings of the CSF flow *in vivo,* we decided to obtain these encodings from a healthy volunteer before starting this study. As shown in Fig. 1, the CSF flows were clearly demonstrated with 6.0 cm/sec, 9.0 cm/sec, 12.0 cm/sec, and 15.0 cm/sec. TVFPs showed a similar pattern in all velocity encodings (Fig. 2). Thus, we decided to use 9.0 cm/sec and 15.0 cm/sec in considering varying velocities of the CSF flow.

Calibration on phantom. Phase images of the steady flow phantom are shown in Fig. 3. The correlation between the calculated velocities using MR system and the calibrated velocities using the electromagnetic flow meter are shown in Fig. 4. Phase contrast technique showed reliable quantitation even in the slow flow.

Normal to-and-fro movement of CSF flow. Phase contranst cine MR images clearly demonstrated a to-and-fro movement of the CSF flows in all of the normal volunteers (Fig. 5 a). The CSF flows of the healthy subjects showed a consistent pattern (Fig. 5 b), and were dependent on the cardiac cycle. The cephalic CSF flows continued until 70 msec after the R-wave and then the flows were reversed to caudal. The CSF flows reached maximum velocity at 190 msec and then the flow reversed again to cephalic. The same turn appeared in the subsequent phase, but then the amplitude decreased. The mean maximum velocity of the CSF flow was 46.6 ± 1.3 mm/sec (mean $\pm$ SEM) and the amplitude was 74.1 ± 3.6 mm. The maximum velocities of the cranial to caudal CSF flows were lower than 9.0 cm/sec in all subjects.

Hydrocephalic To-and-Fro Movement of CSF Flow

Before shunting operation. The patterns of the CSF flow in the patients with NPH were variable and could be divided into following types: type 0 (normal flow pattern)(n = 1), the pattern of the CSF flow was similar to that of the healthy subjects (Fig. 6 a); type I (mildly disturbed flow pattern)(n = 2), the caudal peak flow was delayed later than 190 msec on TVFP and the amplitude was slightly lower than the normal flow pattern (Fig. 6 b); type II (moderately disturbed flow pattern)(n = 6), the caudal peak flow was not apparent (Fig. 6 c), but the

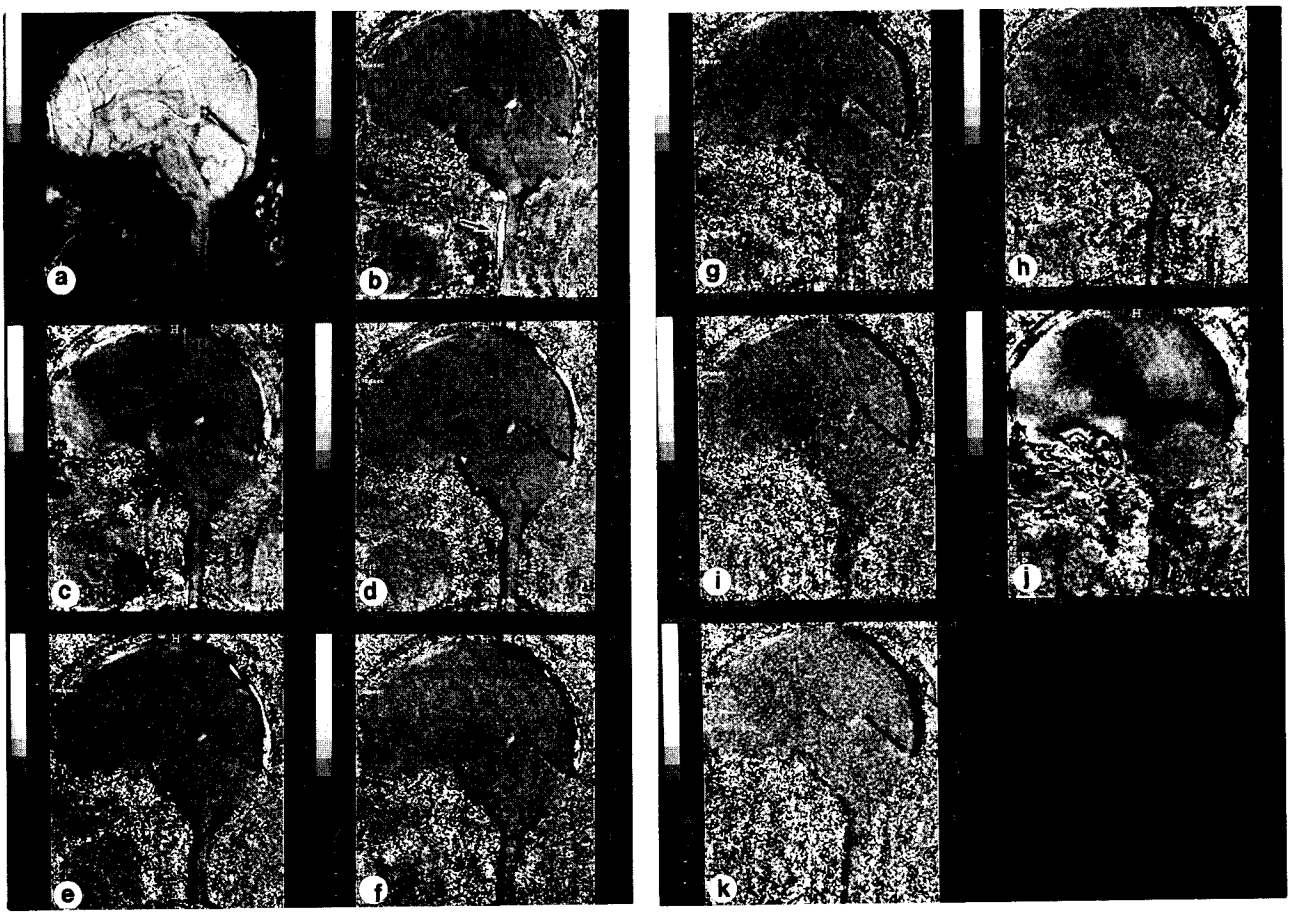

Fig. 1

Fig. 1 A scout view of the midsagittal plane (**a**) and phase images of the brain and the upper cervical spine using 10 degrees of the velocity encodings in a healthy 23-year-old man (**b**-**k**). The velocity encodings ranged from 3.0 cm/sec to 30.0 cm/sec. All images were acquired at 190 msec after the R-wave on ECG. In this cardiac phase, the CSF flow was directed to caudal. The cephalic CSF flow (arrow) is demonstrated, because the phase shifts caused by the actual velocities were more than $-\pi$ (**b**). **b**, 3.0 cm/sec; **c**, 6.0 cm/sec; **d**, 9.0 cm/sec; **e**, 12.0 cm/sec; **f**, 15.0 cm/sec; **g**, 18.0 cm/sec; **h**, 21.0 cm/sec; **i**, 24.0 cm/sec; **j**, 27.0 cm/sec; **k**, 30.0 cm/sec.

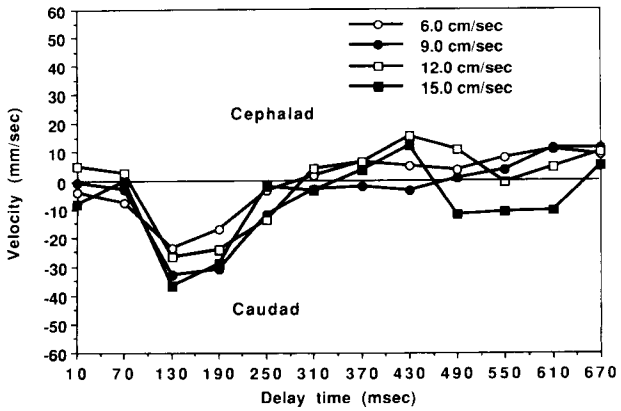

Fig. 2

Fig. 2 The time-velocity flow profiles of the same normal volunteer in Fig. 1 using 6.0 cm/sec, 9.0 cm/sec, 12.0 cm/sec and 15.0 cm/sec as the value of velocity encoding. The CSF velocities were measured in the anterior subarachnoid space at the C2/3 level. Plus velocity (cephalad) mean CSF flow to the rostral direction and minus velocity means the caudal direction of the CSF flow (caudad), These TVFPs showed a similar pattern.

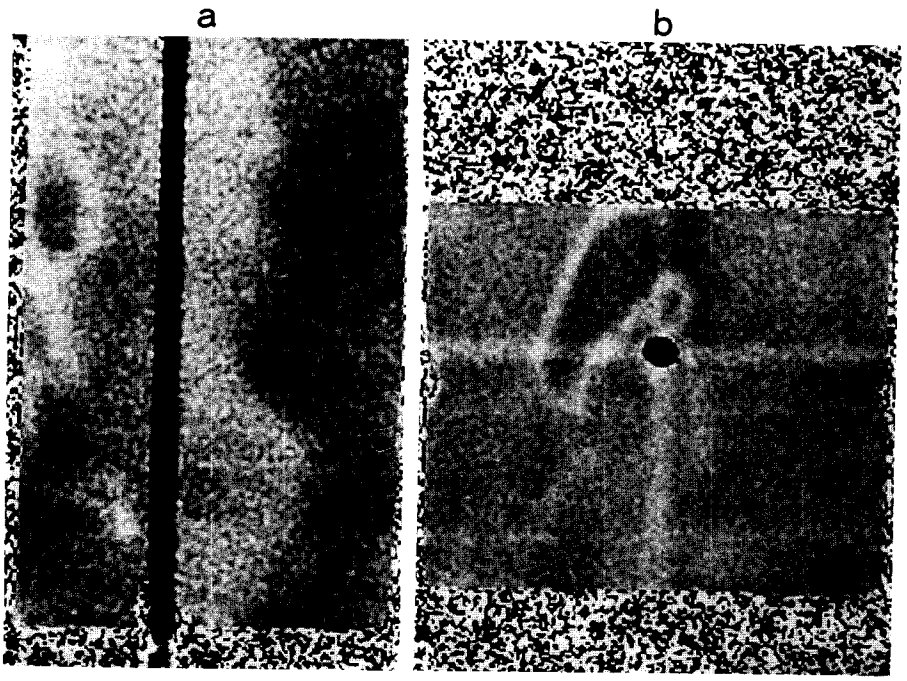

Fig. 3 Phase images of the phantom consisted of the vinyl tube (**a**, black line. **b**, black circle) filled with a saline and the plastic basin (gray rectangle) filled with micromolecular dextran. These images were obtained with a non-gated sequence (120/20/4) (TR/TE/excitations). Flip angle, image matrix, field of view and slice thickness were identical to the cardiac gated sequence.
a: sagittal image. **b**: axial image.

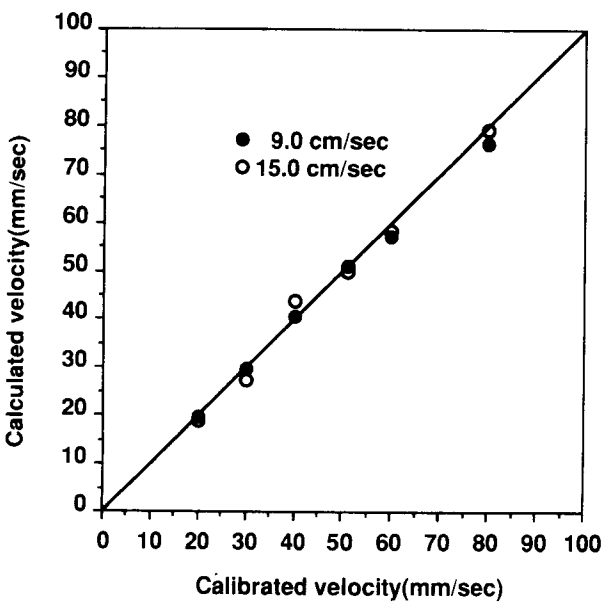

Fig. 4 A correlation between the calculated velocities using MR system and the calibrated velocities using the electromagnetic flow meter was shown using the steady flow phantom. Both velocity encodings show a linear correlation ($r = 0.99$, $p < 0.001$).

CSF flow through the aqueduct was remarkable on phase images (Fig. 7); type III (severely disturbed flow pattern) ($n = 11$), the amplitude of TVFP was very small and the CSF flow through the aqueduct was not identified (Fig. 6 d). The caudal maximum velocities of each type were: type 0, 51.9 mm/sec; type I, 41.1 mm/sec (mean); type II, 30.6 ± 1.3 mm/sec (mean $\pm$ SEM); and type III, 11.8 ± 1.6 (mean $\pm$ SEM). In hydrocephalic conditions, the amplitude of the to-and-fro movement of CSF flow gradually decreased. The decrease in the amplitude of the caudal flow in the systolic phase of the cardiac cycle was most prominent.

Clinical assessment. We measured the NPH score to evaluate the clinical disabilities of the patients with NPH. NPH scores showed a statistically significant correlation to the amplitudes of to-and-fro movement of the CSF flow (Fig. 8 a). NPH scores decreased along with the decrease in the CSF pulsations. Lumbar CSF pressure tended to be high in the patients of type III TVFP, but failed to reach a statistically significant level (Fig. 8 b). Evans' index had no correlation to the amplitudes of CSF pulsations. The mean amplitude of TVFPs

Fig. 5 a

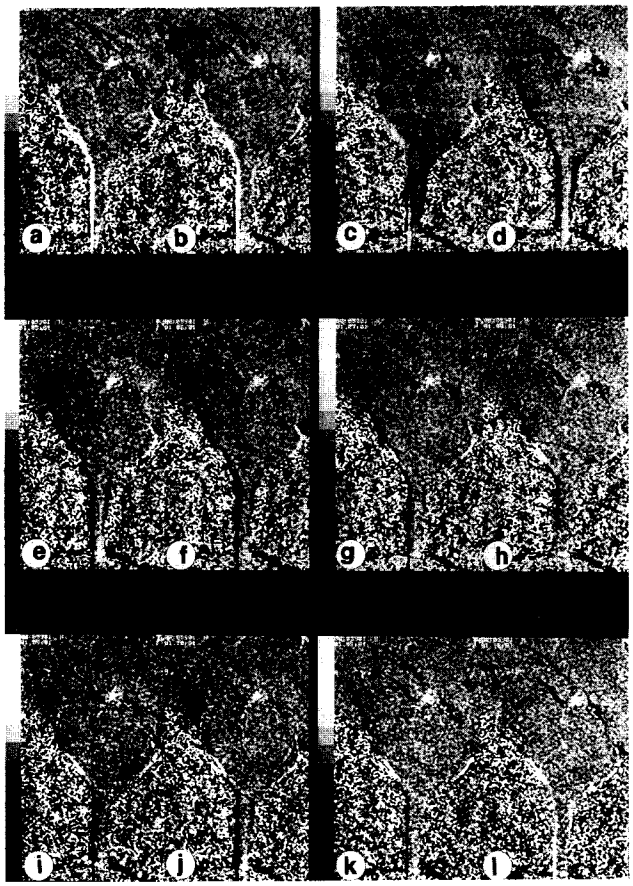

Fig. 5 a Phase images of the brain and the upper cervical spine in a healthy 26-year-old man (**a-l**). Phase images clearly demonstrate to-and-fro movement of the CSF flow in the subarachnoid space anterior to the brainstem and the upper cervical spine. The iso-high signal intensities show the cephalic CSF flow and the iso-low signal intensities show the caudal CSF flow. **a**, 10 msec; **b**, 70 msec; **c**, 130 msec; **d**, 190 msec; **e**, 250 msec; **f**, 310 msec; **g**, 370 msec; **h**, 430 msec; **i**, 490 msec; **j**, 550 msec; **k**, 610 msec and **l**, 670 msec after the R-wave on ECG.

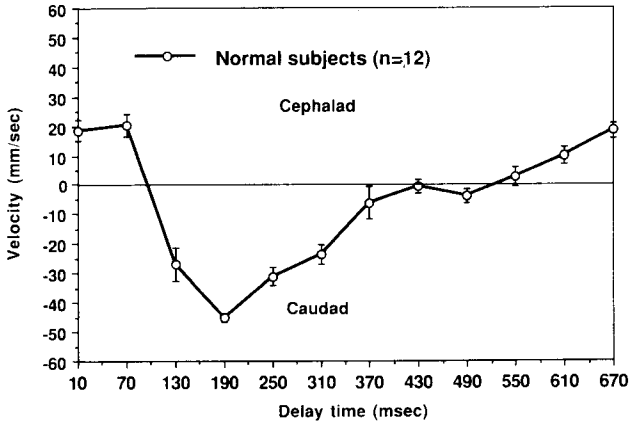

Fig. 5 b The time-velocity flow profiles of the 12 normal volunteers using a 9.0 cm/sec-velocity encoding are shown. These TVFPs show a consistent pattern. The cephalic CSF flow continued until 70 msec after the R-wave and the flow reversed to caudal. The caudal CSF flow reached the maximum velocity (46.6 ± 1.3 mm/sec) at 190 msec and then the flow reversed again to cephalic. Values are means ± SEM.

Table 2 Summary of cases with shunting operation

Case No.	Age /Sex	TVFP			NPH score			
		Type	Amplitude		GE	CF	SD	Total score
		pre / post	pre / pont	% change	pre / post	pre / post	pre / post	pre / post
3	65/M	I / I	56.8 / 81.7	+ 44	2 / 2	2 / 3	1 / 4	5 / 9
7	74/F	II / I	63.7 / 73.9	+ 16	1 / 1	2 / 3	1 / 5	4 / 9
8	64/M	II / I	42.4 / 92.9	+119	2 / 4	3 / 5	1 / 5	6 / 14
9	69/M	II / II	30.3 / 39.4	+ 30	1 / 1	2 / 3	1 / 3	4 / 7
11	65/F	III / III	14.0 / 18.5	+ 32	1 / 1	2 / 3	1 / 2	4 / 6
12	72/F	III / —	13.7 / —	—	1 / 1	3 / 4	1 / 3	5 / 8
13	44/F	III / II	25.4 / 39.7	+ 56	1 / 1	2 / 3	1 / 5	4 / 9
14	43/M	III / II	22.6 / 58.5	+159	2 / 4	2 / 4	1 / 5	5 / 13
15	74/F	III / III	14.1 / 24.8	+ 76	1 / 1	2 / 3	1 / 1	4 / 5
16	46/M	III / 0	11.7 / 88.0	+652	1 / 4	2 / 3	1 / 2	4 / 9
17	57/M	III / III	17.5 / 15.4	− 12	1 / 1	2 / 2	1 / 1	4 / 4
18	70/F	III / III	27.9 / 16.9	+ 39	1 / 1	2 / 2	1 / 1	4 / 4
19	66/F	III / I	23.8 / 84.6	+255	1 / 1	2 / 4	1 / 2	4 / 7
20	78/F	III / I	27.4 / 69.9	+155	2 / 2	3 / 3	3 / 5	8 / 10

GE: gait evaluation, CF: congnitive function, SD: sphincter disturbance
TVFP: time-velocity flow profile

in the patients with PVL was 36.9 ± 6.5 mm (mean ± SEM) and that in the patients without PVL was 32.9 ± 6.7 mm. No statistically significant difference in the amplitude of TVFP was found between the patients with PVL and those without PVL.

After shunting operation. Fourteen of the 20 patients with NPH were shunted. Postoperative images were obtained in 13 patients who were shunted. Elven of these 13 patients were responsive to shunt therapy and 2 patients (Case 17 and 18) were not responsive (Tab. 2). The amplitude of TVFP increased in 11 of the patients who improved clinically after the shunting operation. Five of the type III cases changed to type II (Cases 13 and 14) (Fig. 9 a), type I (Case 19 and 20) and type 0 (Case 16) (Fig. 9 b) and also one of the type II cases improved to type I (Case 8) after the shunting operation. However, the amplitude of TVFP decreased in 2 patients who were unchanged clinically after the shunting operation. The ventricular catheter was obstructed in case 17 and the malfunction of the shunt valve ocurred in case 18.

Discussion

Measurement of CSF flow velocity by phase contrast cine MR imaging. Although the phase contrast technique proved to be reliable method of measurement for the steady flow phantom, there were some problems in the practical study. The most important problem was in the selection of the sensitive velocity encoding. If the velocity encoding was not adequate for the actual velocity, we could not accurately measure the velocity. When the

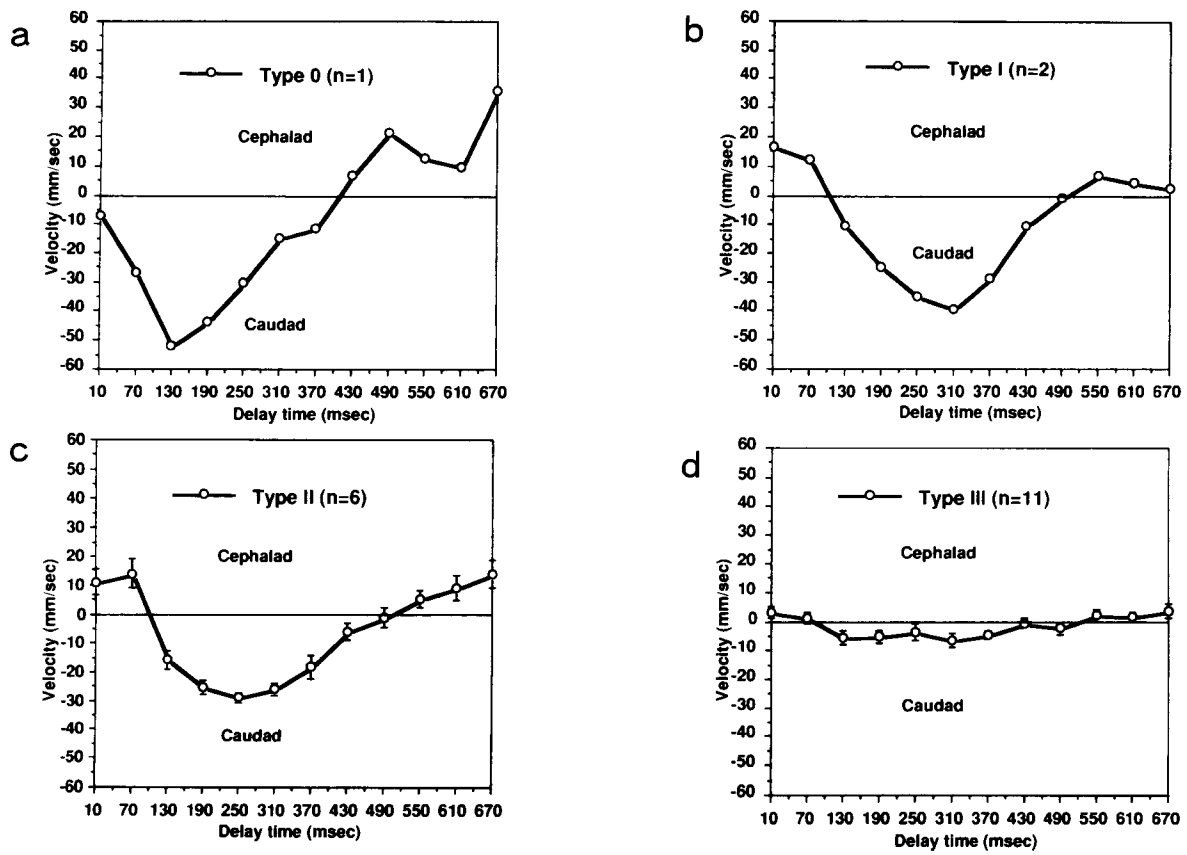

Fig. 6 Time-velocity flow profile of the patients with types 0, I, II and III. a: The TVFP of the patient with type 0 was similar to that of normal subjects. b: The TVFP of the patient with type I was also similar to that of normal subjects. However, the caudal peak flow appeared later than 190 msec after the R-wave and that the amplitude slightly decreased compared with normal TVFP. c: The caudal peak flow was not apparent in the TVFP type II. d: The amplitude of the CSF pulsatile flow decreased in the TVFP type III

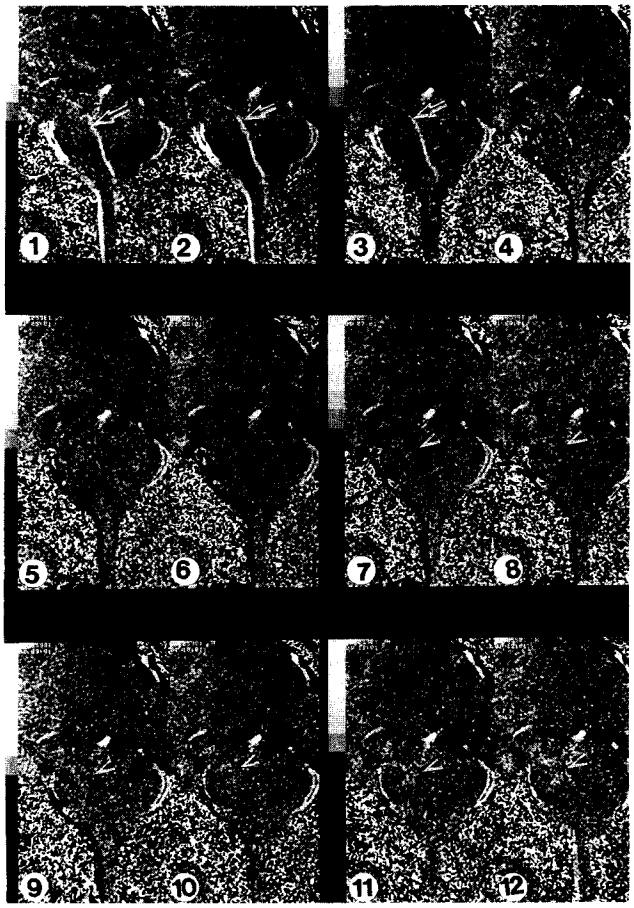

Fig. 7 (Left) Phase images (sequential 12 images) of the patients with type II TVFP. These images show the cephalic CSF flow (arrows) and the caudal CSF flow (arrow heads) through the aqueduct.

Fig. 8 (Bottom) a: The correlation between NPH scores and the amplitudes of to-and-fro movement of CSF flow shows a statistical significance ($r = 0.50$, $p < 0.05$). b: The lumbar CSF pressures were higher in the patients with type III TVFP than others, but failed to reach statistically significant level ($r = 0.28$, $p < 0.3$). Black circles are Types 0, I and II.

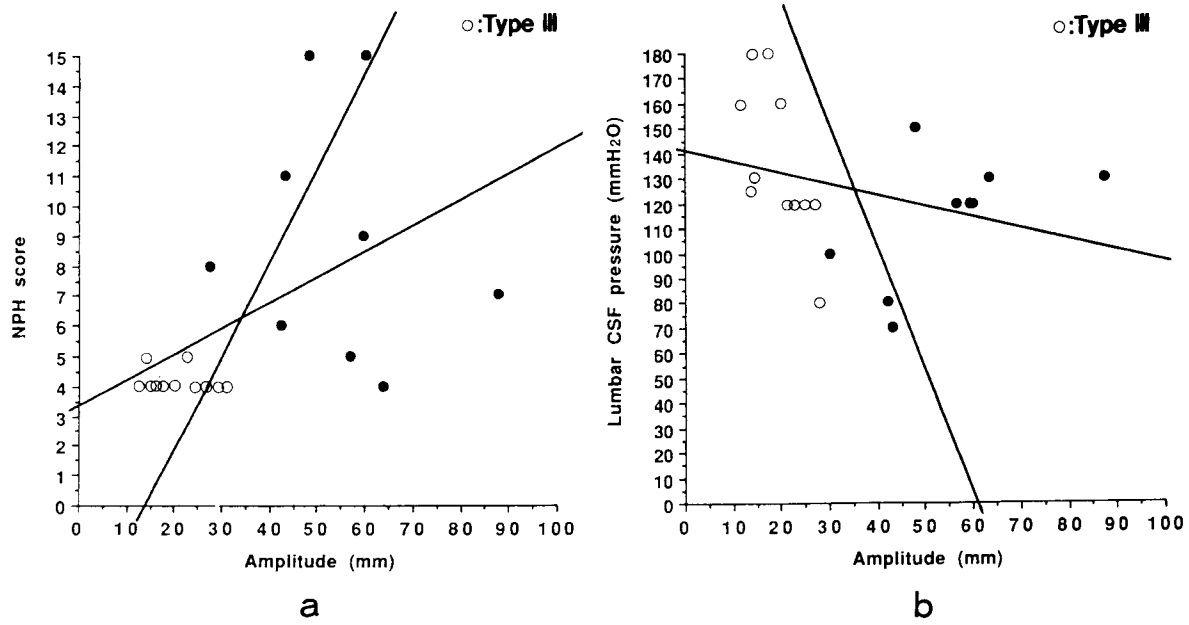

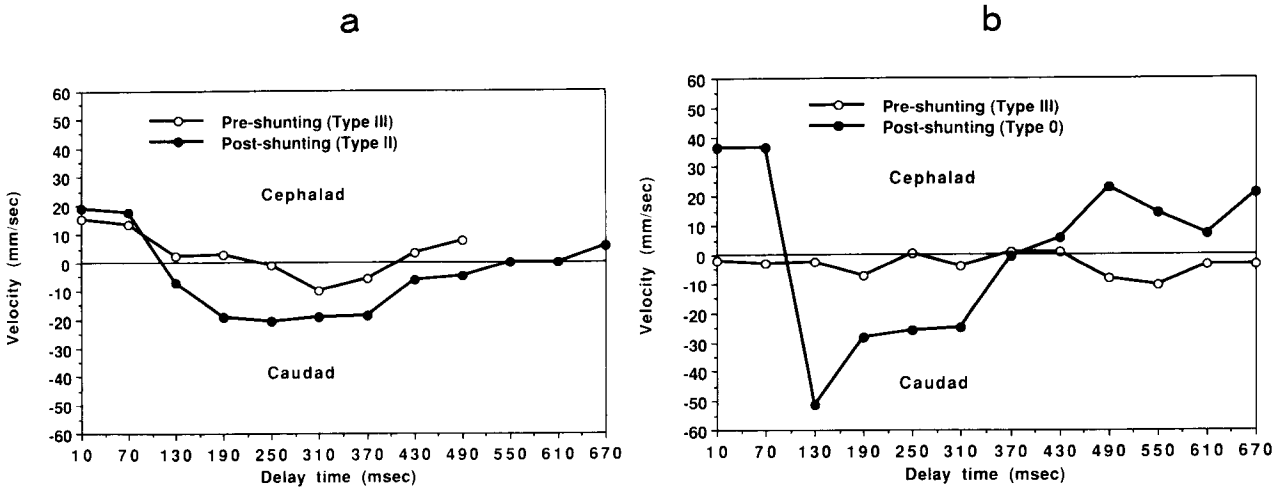

Fig. 9 Time-velocity flow profiles of patients before and after the shunting operation. a: Case 13. Two weeks after the shunt, the CSF flows in the anterior subarachnoid space increased and the amplitude of the caudal CSF flow also increased on TVFP. b: Case 16. Note the normal flow profile after the shunt.

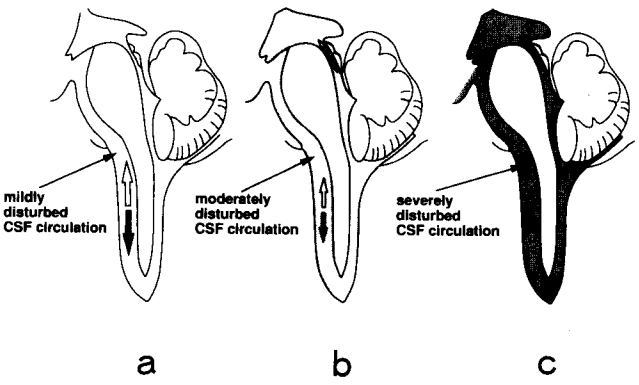

Fig. 10 Schematic illustrations of the to-and-fro movement of CSF flow in each NPH type. When the disturbance of the CSF absorption was mild, the to-and-fro movement of CSF flow keeps a relatively large amplitude (a). When the CSF circulation is moderately disturbed due to increased resistance to absorption of CSF, the CSF flow volumes in the ventricular system increase. Consequently, the CSF flows through the aqueduct increase. Thus, the CSF flows through the aqueduct on phase images are apparent (b). However, when the CSF flows are severely disturbed, the amplitudes of to-and-fro movement of CSF flow become very small. In this condition, the effective pulsation which drive the increased CSF volvme in the ventricular system is lacking. Then the velocities of CSF flow through the aqueduct decrease and the detection of CSF flow by a 9.0 cm/sec-velocity encoding become poor. Therefore, the CSF flows through the aqueduct on phase images are not identified (c). Additionally, the aqueduct was not parallel to the bipolar flow-encoding gradient pulse. This also produced a poor detection of the CSF flow through the aqueduct compared with that in the anterior subarachnoid space. White arrow represents the cephalic CSF flow and black arrow represents the caudal CSF flows. a, Type 0, I; b, Type II; c, Type III.

actual velocities were higher than the velocity encoding and the phase shifts caused by one bipolar pulse were more than $\pm \pi/2$, the signal intensties were decreased. Furthermore, when the phase shifts was more than $\pm \pi$, the signal intensities were reversed. Other problems were the effects of eddy currents. These effects did not vanish completely on general subtraction and produced phase errors. These phase errors were corrected on a specific subtraction process in our MR system. Furthermore, we subtracted the signal intensity of the background from that of the ROI to reduce the effects on eddy currents when we calculated the flow velocities. Phase dispersions induced by the different flow velocities in a voxel produced phase errors and decreased the signals. In this study, we made the voxel as small as possible in order to reduce the phase dispersions.

Normal CSF flow pattern. As a mechanism of the to-and-fro motion of the CSF flow, Du Boulay (30) described the squeezing of the thalami and Bering (31) explained the expansion of the choroid plexus. Feinberg (32) described that the CSF pulsation depended on the cardiac cycle as follows. During the systolic phase, an inward force directed from the cerebral cortex inside the brain was produced by expansion of the cerebral arterial vessels and this increased the pressure in the lateral ventricles. Consequently, the CSF in the lateral ventricles was pushed out and in addition, a brainstem motion

directed to caudal drove the CSF into the spinal. Our study also showed that the pattern of the CSF flow depended on the cardiac cycle. Itabashi (33) reported a similar pattern of the CSF flow at the upper cervical spine using velocity density method. He indicated that the caudal maixmum velocities were 26-44 mm/sec at the upper cervical and 44-124 mm/sec at the lower cervical level. He thought that this differnce was caused by individual morphological differences and differences in the neck position. These individual morphological differences affected the calibrated velocities. In fact, the calibrated velocities of the healthy subjects showed some differences, but the pattern of the normal CSF flow was consistent.

Hydrocephalic CSF flow pattern. Previous MR studies (21-29) have shown that the CSF flow-void signs in the aqueduct increased in hydrocephalic conditions. Although many factors affect the pathophysiology of NPH, increased resistance to the absorption of CSF and decreased compliance of the craniospinal CSF cavity have been cited as important factors (16). When the CSF absorption is disturbed by subarachnoid adhesions secondary to subarachnoid hemorrhage or inflammation, the CSF volume in the ventricular system increases. Increased CSF volume and decreased compliance are considered to increase the CSF flow-void signs.

The CSF flows through the aqueduct on phase images were observed only in the patients of type II. Although the slice thickness was 5 mm in the present study, the diameter of the aqueduct was considered to be approximately 1 mm in the healthy subject. Consequently, the excited slab included a large number of stationary protons of brain tissue compared with the moving protons through the aqueduct. Therefore, the signals from the moving protons through the aqueduct were too small to be detected in the healthy subjects. The same mechanism was considered to function in the patients of type 0 and type I who demostrated normal or mildly disturbed CSF flow pattern. When the CSF circulation was moderately disturbed, the CSF flow volumes in the ventricular system and through the aqueduct increased due to the increased resistance to the absorption of CSF. The signals from the moving protons through the aqueduct were also greater than the signals from the stationary protons. Thus, the CSF flows through the aqueduct on phase images were observed in the patients of type II. However, when the CSF flows were severely disturbed, the amplitudes of the CSF pulsatile flows became very small. In this condition, the velocities of CSF flows through the aqueduct decreased because the effective pulsation which drove the increased CSF volume in the ventricular system was lacking. Therefore, the CSF flows though the aqueduct on phase images were not identified in the patients of type III (Fig. 10).

Clinical assessment before and after shunting procedure. The amplitude of to-and-fro movement of the CSF flow decreased with the decrease of NPH score in the present study. It was interesting to note that some of the patients showed Type 0 TVFP or Type I TVFP. Their CSF flow patterns were similar to the normal flow patters in the present study. These facts suggest that the disturbance of to-and- fro movement of CSF flow certainly affects the pathophysiology of NPH, but is not an only factor.

In the present study, improvement rates in the clinical symptoms after the shunting operation were as follows: gait disturbance, 21.4 %; dementia, 85.7 %; urinary incontinence, 78.6 %. NPH score improved most significantly in urinary incontinence (average of 2.5 points). Thus, we can expect a most prominent recovery in urinary incontinence at an early period after the shunting operation. Because most of the patients were bedridden before shunting operation, we needed a longer time between the operation and the postoperative MR imaging to evaluate the improvement in gait distubrance.

Shunt therapy and shunt patency. Although Adams and Hakim (11) described NPH as a surgically treatable dementia, it has been difficult to decide whether a patient is shunt-responsive or not before the operation. Accordingly, the patients of type III were of interest because they showed low amplitudes of the to-and-fro movement of the CSF flows and low NPH scores. Amplitude of the CSF pulsation decreased as NPH score decreased in the present study. If this process is reversible (*i. e.* the amplitude increases again with the increase of NPH score by shunting operation), we can expect a most favorable outcome in the patients of type III. Postoperative examinations in the present study support this idea.

Five of the type III cases changed to types II, I and 0 and one of the type II cases changed to type I after the shunting operation. This fact shows a transitional change in each type and its reversibility by shunting operation. Therefore, we are able to assess the shunt patency by comparing TVFP before and after the shunting operation. When a patient neither improves clinically nor shows an increase in the amplitude of TVFP after shunting opera-

tion, shunt malfunction should be considered. When a patient does not improve clinically in spite of the improvement in the CSF pulsation by shunt therapy, brain tissue damages caused by disturbance of the CSF circulation have already become irreversible or one should consider the existence of other pathophysiology, such, as Alzheimer disease or Binswanger disease.

Borgesen *et al.* (34), using a continuous monitoring of ICP, demonstrated that the combination of low compliance of the brain and high resistance to outflow of CSF (R out) may be necessary to produce the B-wave and to be beneficial after the shunting procedure. Kosteljanetz (35) showed a positive correlation between the abnormally raised R out and ICP. In the present study, lumbar CSF pressure were certainly high in the patients of type III, but not statistically significant. However, we suspect that the decrease in the CSF pulsation correlates with ICP. Transient elevation of ICP in the patients with NPH has been reported using continuons monitoring of ICP (13, 15, 36, 37). When this continuous monitoring is applied , a significant correlation between the decrease of CSF pulsation and the increase of ICP may be found. We consider that the most beneficial effect of shunting is expected in the patients of type III and that the effect of shunting is less in other types. All the patients of type III should be shunted, because they have low CSF pulsation amplitudes which correlates with clinical feature. In other types, when the clinical symptoms are very progressive or the progress of disturbance of CSF circulation is shown by the repeat phase contrast cine MR imaging, the shunt operation should be performed.

Phase contrast cine MR imaging is useful for the quantitative analysis of the CSF flow. We believe that our study is valuable for the clinical assessment of NPH and preselecting shunt-responsive patients will be possible using phase contrast cine MR imaging.

Acknowledgments. The authors thank Dr. Takahiko Itoh, Dr. Shohei Tsuchida, Dr. Kazushi Kinugasa and all the staff of the Department of Radiology, Kohsei Hospital who have helped in this study.

References

1. Dumoulin CL and Hart,Jr HR: Magnetic resonance angiography. Radiology (1986) **161**, 717-720.
2. Dumoulin CL, Souza SP and Feng H: Multiecho magnetic resonance angiography. Magn Reson Med (1987) **5**, 47-57.
3. Dumoulin CL, Souza SP and Hart HR: Rapid scan magnetic resonance angiography. Magn Reson Med (1987) **5**, 238-245.
4. Dumoulin CL, Souza SP, Walker MF and Yoshitome E: Time-resolved magnetic resonance angiography. Magn Reson Med (1988) **6**, 275-286.
5. Dumoulin CL, Souza SP, Walker MF and Wagle W: Three-dimensional phase contrast angiograhy. Magn Reson Med (1989) **9**, 139-149.
6. Walker MF, Souza SP and Dumoulin CL: Quantitative flow measurement in phase contrast angiography. J Comput Assist Tomog (1988) **12**, 304-313.
7. Itoh T, Katayama S, Tsuchida S, Asari S, Nishimoto A, Doi A, Yoshioka J, Ikezaki Y and Yoshitome E: Magnetic resonance angiography by a phase contrast method using a 0.5T imager: The conditions for imaging intracranial vessels. Jpn Magn Reson Med (1990) **10**, 510-520 (in Japanese).
8. Pernicone JR, Siebert JE, Potchen EJ, Pera A, Dumoulin CL and Souza SP: Three-dimensional phase-contrast MR angiography in the head and neck: Preliminary report. Am J Neuroradiol (1990) **11**, 457-466.
9. Enzmann DR and Pelc NJ: Normal flow patterns of intracranial and spinal cerebrospinal fluid defined with phase-contrast cine MR imaging. Radiology (1991) **178**, 467-474.
10. Pettigrew RI, Dannels W, Galloway JR, Pearson T, Millikan W, Henderson JM, Peterson J and Bernardino ME: Quantitative phase-flow MR imaging in dogs by using standard sequences: Comparison with *in vivo* flow-meter measurements. Am J Radiol (1987) **148**, 411-414.
11. Adams RD, Fisher CM, Hakim S, Ojemann RG and Sweet WH: Symptomatic occult hydrocephalus with normal cerebrospinal fluid pressure: A treatable syndrome. N Engl J Med (1965) **273**, 117-126.
12. Shenkin HA, Greenberg JO and Grossman CB: Ventricular size after shunting for idiopathic normal pressure hydrocephalus. J Neurol Neurosurg Psychiatry (1975) **38**, 833-837.
13. Crockard HA, Hanlon K, Duda EE and Mullan JF: Hydrocephalus as a cause of dementia: Evaluation by computerized tomography and intracranial pressure monitoring. J Neurol Neurosurg Psychiatry (1977) **40**, 736-740.
14. Gunasekera L and Richardson AE: Computerized axial tomography in idiopathic hydrocephalus. Brain (1977) **100**, 749-754.
15. Symon L and Dorsch NWC: Use of long-term intracranial pressure measurement to assess hydrocephalic patients prior to shunt surgery. J Neurosurg (1975) **42**, 258-273.
16. Sahuquillo J, Rubio E, Codina A, Molins A, Guitart JM, Poca MA and Chasampi A: Reapprasial of the intracranial pressure and cerebrospinal fluid dynamics in patients with the so-called "normal pressure hydrocephalus" syndrome. Acta Neurochir (Wien)(1991) **112**, 50-61.
17. Vorstrup S, Christensen J, Gjerris F, Soressen PS, Thomsen AM and Paulson OB: Cerebral flow in patients with normal-pressure hydrocephalus before and after shunting. Neurosurgery (1987) **66**, 379-387.
18. Sherman JL and Citrin CM: Magnetic resonance demonstration of normal CSF flow. Am J Neuroradiol (1986) **7**, 3-6.
19. Sherman JL, Citrin CM, Gangarosa RE and Bowen BJ: The MR appearance of CSF pulsations in the spinal canal. Am J Neuroradiol (1986) **7**, 879-884.
20. Citrin CM, Sherman JL, Gangarosa RE and Scanlon D: Physiology of the CSF flow-void sign: Modification by cardiac gating. Am J Neuroradiol (1986) **7**, 1021-1024.
21. Bradley WG, Kortman KE and Burgoyne B: Flowing cerebrospinal fluid in normal and hydrocephalic states: Appearance of MR images. Radiology (1986) **159**, 611-616,
22. Mascalchi M, Ciraolo L, Tanfani G, Taverni N, Inzitari D, Siracusa GF

and Pozzo GCD: Cardiac-gated phase MR imaging of aqueductal CSF flow. J Comput Assist Tomogr (1988) **12**, 923-926.
23. Ohara S. Nagai H, Suzaka T, Matsumoto T and BannoT: Observatiom of the CSF pulsatile flow on MRI (2)-The signal-void phenomenon and its relation to the intracrasial pressure. Prog Comput Tomogr (1988) **10**, 5-12 (in Japanese).
24. Ohara S, Nagai H, Matsumoto T and Banno J: MR Imaging of CSF pulsatory flow and its relation to intracranial pressure. J Neurosurg (1988) **69**, 675-682.
25. Toyoda T, Eguchi T, Iai S, Hibi T, Kawamoto S, Yano M, Ouchi T and Umeda M: Measurement of the CSF velocity using cine mode MRI. Prog Comput Tomogr (1989) **11**, 297-305 (in Japanese).
26. Mascalchi M, Ciraolo L, Bucciolin M, Inzitari D, Arnetoli G and Pozzo GD: Fast multiphase MR imaging of aqueductal flow: 2. Study in patients with hydrocephalus. Am J Neuroradiol (1990) **11**, 597-603.
27. Nakajima S, Maruyama T, Azuma S, Shimura F, Hoshi E, Yoshida E, Matsuura H, Kimura T and Miwa T: Observation of the CSF pulsative flow using cine MRI and presaturation pulse: First report. Prog Comput Tomog (1990) **12**, 277-296 (in Japanese).
28. Quencer RM, Donovan Post MJ and Hinks RS: Cine MR in the evaluation of normal and abnormal CSF flow: Intracranial and intraspinal studies. Neuroradiology (1990) **32**, 371-391.
29. Bradley WG, Whittemore AR, Kortman KE, Watanabe AS, Homyak M, Teresi LM and Davis SJ: Marked cerebrospinal fluid void: Indicator of successful shunt in patients with suspected normal-pressure hydrocephalus. Radiology (1991) **178**, 459-466.
30. Du Boulay GH, O'Connell J, Currie J, Bostick T and Verity P: Further investigation on pulsatile movements in the cerebrospinal fluid pathways. Acta Radiol Diagn (1972) **13**, 496-523.
31. Bering RA: Circulation of the cerebrospinal fluid: Demonstration of the choroid plexuses as the generator of the force for flow of fluid and ventricular enlargement. J Neurosurg (1962) **19**, 405-413.
32. Feinberg DA and Mark AS: Human brain motion and cerebrospinal fluid circulation demonstrated with MR velocity imaging. Radiology (1987) **163**, 793-799.
33. Itabashi T: Quantitative analysis of cervical cerebrospinal fluid and syrinx fluid pulsations. J Jpn Orthop Assoc (1990) **159**, 611-616.
34. Brogesen SE, Gjerris F and Sorensen SC: Cerebrospinal fluid conductance and compliance of the craniospinal space in normal-pressure hydrocephalus. J Neurosurg (1979) **51**, 521-525.
35. Kosteljanetz M: Intracranial pressure: Cerebrospinal fluid dynamics and pressure-volume relations. Acta Neurol Scand [Suppl] (1987) **111**, 1-23.
36. Chawla JC, Hulme A and Cooper R: Intracranial pressure in patients with dementia and communicating hydrocephalus. J Neurosurg (1974) **40**, 376-380.
37. Hartmann A and Alberti E: Differentiation of communicating hydrocephalus and presenile dementia by continuous recording of cerebrospinal fluid pressure. J Neurol Neurosurg Psychiatry (1977) **40**, 630-640.

Received September 3, 1992; accepted December 28, 1992.